EFFECT OF HYDROGEN ON FRACTURE MORPHOLOGY OF HYDROGEN ASSISTED CRACKING IN STEEL WELDMENTS.

N. ALAM, H. LI, L. CHEN and D. DUNNE
Department of Materials Engineering, University of Wollongong, Australia.

ABSTRACT

The interaction of hydrogen and residual stress in a susceptible microstructure in a steel weldment promotes hydrogen assisted cold cracking (HACC). Hydrogen is commonly believed to accumulate in triaxially stressed regions during an incubation period in which the concentration of hydrogen builds up and eventually exceeds a critical amount, resulting in the opening up and propagation of cracks through the weldment. For high hydrogen electrodes, cracking in the weldment can occur in a very short period of time as the supply of hydrogen is abundant. The fracture morphology can be the result of quasi-cleavage (QC) or microvoid coalescence (MVC) or a combination of both. In the present work the microstructures and fracture morphologies of cold cracks developed in weldments produced by deposition of high and low hydrogen electrodes onto 550 MPa (80 ksi) base plate steels were investigated to elucidate the mechanism of fracture with respect to possible hydrogen accumulation sites and the structural sources of crack initiation and easy propagation.

Weldments from low hydrogen electrodes exhibited delayed cracking which was found to initiate in the heat affected zone (HAZ) by intergranular (IG) fracture. Cracking in the weld metal of high hydrogen cellulosic electrodes was found to be both transgranular and intergranular (or intercolumnar, IC). In the case of IG fracture, the crack path was along the prior austenite grain boundaries in the HAZ and through the veins of allotriomorphic ferrite decorating the columnar grain boundaries in the weld metal. In contrast, the transgranular cracking was mainly quasi-cleavage for the HAZ and ductile for the weld metal, consisting of small coalesced microvoids. Fine non-metallic inclusions were present in the fusion boundary and were associated with the initiation of the microvoids ahead of the advancing crack tip.

KEYWORDS

Hydrogen, crack initiation and propagation, weld metal, heat affected zone, fracture, microvoid coalescence mode, cleavage mode, stress concentration.

1. INTRODUCTION

Cold cracking in steel weldments is a crucial factor which limits the application of high strength low alloy steels in structural applications. In the last few decades the weldability of high strength structural steels has increased significantly by improved steel design and processing techniques. This improvement in strength and weldability can offer significant reductions in steel and fabrication costs. Although improved steel design minimises the risk of cold cracking in the HAZ, cracking in strength matching weld metals has became an issue because of their relatively poor HACC resistance, particularly for welding at low heat inputs without hydrogen controlled procedures.

HACC is considered [1] to occur when the following four conditions are present simultaneously:

1) a critical concentration of diffusible hydrogen at a crack tip,
2) a stress intensity at the crack tip of sufficient magnitude,
3) a microstructure susceptible to cracking, and
4) a temperature lower than about 200 °C.

During weld solidification hydrogen is trapped and diffuses into regions of high stress concentration. The critical hydrogen concentration necessary for cracking to occur is a function of the stress and also of the microstructure, which can greatly influence the susceptibility to hydrogen cracking. It is well recognised that twinned martensite exhibits greater susceptibility to HACC than lath martensite [2,3], whereas bainitic ferrite containing sheaves of narrow, parallel ferrite laths has a lower susceptibility to HACC, with autotempered low carbon martensite and granular bainite being least embrittled by hydrogen [2-4].

The mechanism of HACC has been described by many theories, but no single theory can currently explain all of the experimental results. However, it is generally agreed that hydrogen diffuses to the interface of ferrite and carbide in a susceptible microstructure which is relatively hard and possesses low toughness. The stresses resulting from a severe weld thermal cycle are relaxed in hard microstructures either by the opening up of microcracks at the sites of high hydrogen concentration or by initiating cracks in stress concentrated regions. The stress intensity is then relaxed by fracture through the weld.

The fracture morphology of hydrogen assisted cracks can be influenced by the total hydrogen present in the weld. For a self-restrained cracking test, a high concentration of hydrogen in the HAZ has been found to initiate cracking by MVC [5] and for a low hydrogen concentration the cracking may initiate by IG at the same stress level [6]. Similar information for cracking in the weld metal is not available. In an attempt to establish appropriate strength matching electrodes for X80 and HSLA80 steels, which are regarded as highly weldable steels, cold cracked weld metals from low and high hydrogen electrodes were examined to characterise the fracture morphology of HACC for better understanding of the cracking mechanism in the weld metal.

2. EXPERIMENTAL

Study of HACC of weld metal was carried out on X80 and HSLA80 steels using the RRC and Tekken tests, respectively. Both tests were instrumented to detect the occurrence of cracking. The thermal profile was recorded from an embedded thermocouple. Following the tests the hardness of weld metal was measured and microstructural and fractographic analyses were carried out. The chemical analyses of the two steels and associated weld metals are given in Table 1.

2.1 RRC Testing

The HACC testing was conducted on 9 mm thick X80 steel by BHP-FPD. A single pass weld was deposited using an E9010 electrode, which is a high hydrogen potential (32 ml/100g) cellulosic electrode. A heat input of 0.65 kJ/mm was used to deposit a 100 mm long weld in a 60° V groove with a small root face.

2.2 Tekken Testing

This form of testing was carried out on a 25 mm thick HSLA80 steel. In this test a single weld was deposited from a low hydrogen (6-8 ml/100g) E8018B2 electrode in a 60° oblique Y groove. A heat input of 1 kJ/mm was used to deposit a 100 mm long weld.

2.2 Crack Analysis

After removal from the test jig samples were sectioned into 10 pieces and prepared for microscopic analysis of the microstructure and the fracture initiation and propagation. Following microstructural analysis, the section was cooled in liquid nitrogen and fractured so that the crack surface caused by HACC could be examined using scanning electron microscopy (SEM).

Table 1: Chemical compositions (wt%) of the X80 and HSLA80 steels and their weld metals.

Steel	C	Mn	Si	Ni	Cr	Mo	Cu	Al	Ti	Nb	V
X80	0.07	1.62	0.33	0.028	0.03	0.22	0.01	0.031	0.013	0.058	0.003
E9010[1]	0.14	1.16	0.19	0.089	0.03	0.19	0.02	0.015	0.013	0.028	0.022
HSLA80	0.06	1.40	0.25	0.85	0.02	-	1.10	-	0.013	0.020	-
E8018B2[2]	0.07	0.80	0.30	-	1.20	0.50	-	-	-	-	-

1: Actual diluted weld metal on X80; 2: Supplier's analysis of the consumable (undiluted).

3. RESULTS

From the sectioned welds, crack initiation and propagation through the weldment were examined with respect to various microstructural features. For fractographic analysis the area examined was very close to the polished and etched section in order to correlate the microstructure with the morphology of the fracture surface.

3.1 Microstructure and Crack Analysis

Typical macroviews of weld sections from the RRC and Tekken tests are shown in Fig. 1. From this figure it is evident that the weld from the RRC test (Fig. 1a) has undercuts near both side-walls of the upper weld metal surface and most cracks were found to initiate from the root of the undercut which corresponded to the smaller throat height. On the other hand, the sample from the Tekken test exhibited a sharp notch at the root (Fig. 1b) which simulates the condition of lack of root penetration. Stresses are concentrated at the root of the Tekken test weld and cracks were found to initiate from the root.

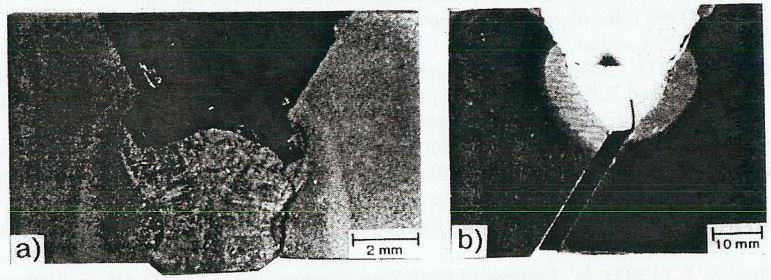

Figure 1: Macroviews of sectioned welds from a) RRC and b) Tekken test samples.

The weld metal formed with the cellulosic electrode (in the RRC test) showed columnar grains which were decorated with pro-eutectoid ferrite allotriomorphs, some with ferrite side plates. The columnar grains contained mainly an acicular ferrite microstructure. Cracks in various regions of the weld metal microstructures are shown in Fig. 2.

Crack initiation occurred typically at the undercut surface of the high hydrogen weld metal across acicular ferrite, Fig. 2a. However, crack propagation was found to be strongly influenced by grain boundary ferrite, which exhibited a low resistance to fracture. Typical crack propagation through pro-eutectoid ferrite along columnar grain boundaries is shown in Fig. 2b. A significant portion of the crack was also found to follow the fusion boundary of the weld, Fig. 2c and the last portion of the crack path was through the HAZ of the X80 steel, Fig. 2d.

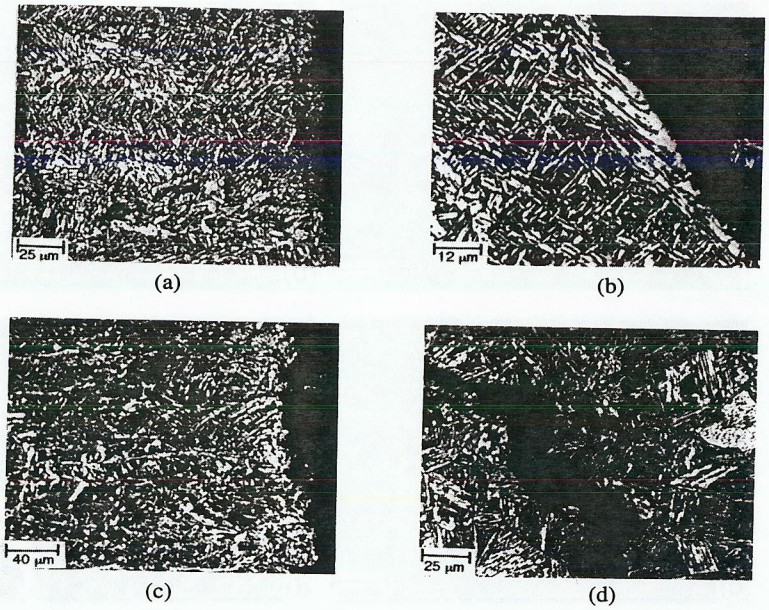

Fig. 2: Photomicrographs of high hydrogen welds obtained in the RRC test: a) crack initiation in acicular ferrite zone across the columnar grains; b) crack propagation along grain boundary ferrite; c) crack propagation along fusion boundary; d) intergranular crack propagation through HAZ.

The microstructure of the weld metal produced with the low hydrogen electrode (in the Tekken test) is shown in Fig. 3. The weld metal consisted mainly of bainitic ferrite with regions of acicular ferrite type structure. There was a trace of ferrite along the columnar grain boundaries. Cracks detected in the low hydrogen weld metal were usually small and often started at the root of the weld by initiating either across the columnar grains of the weld metal or in the HAZ. However, cracks which started in the HAZ were found to propagate in the weld metal.

3.2 Fracture Morphology

SEM micrographs of the cold cracked surface from the cellulosic electrode (X80 welds) are shown in Fig. 4 corresponding to various microstructures. Cracking in all weld metals was found to occur initially by MVC and then by the intercolumnar (IC) mode. Initial cracking occurred in the fine acicular ferrite by void coalescence producing fine dimples, see Fig. 4a. When the crack followed the ferrite veins along the columnar grain boundaries the fracture showed a relatively plane surface consistent with IC (or IG) fracture, with little sign of deformation, see Fig. 4b. Cracks along the fusion boundary were characterised by MVC nucleated by non-metallic inclusions, see Fig. 4c. Cracks in the HAZ were characterised by quasi-cleavage and intergranular type fracture (Fig. 4d).

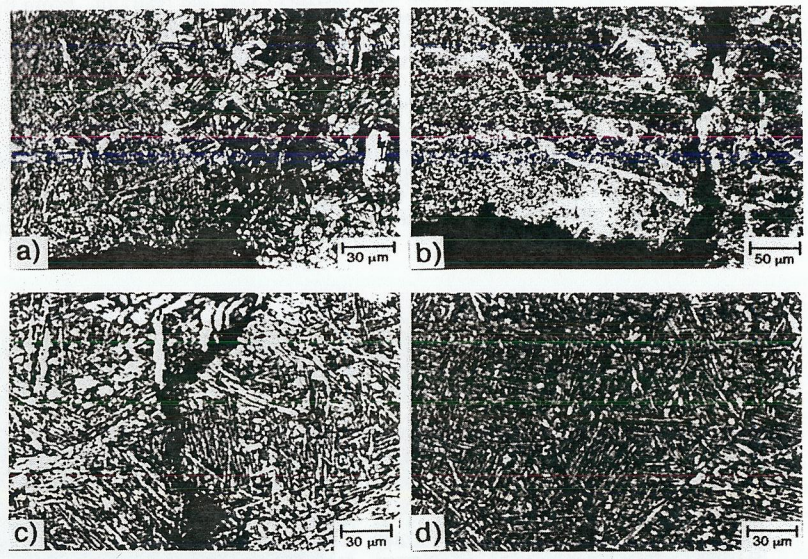

Fig. 3: Photomicrographs of low hydrogen welds obtained in the Tekken test: a) crack initiation (IG) in HAZ; b) crack initiation (QC) in weld metal; c) cracking through bainitic ferrite and along columnar grain boundaries of weld metal; d) crack arrest in acicular ferrite of weld metal.

In the low hydrogen weld metal, cracks were found to initiate by the IG or IC mode. When the crack initiated in the HAZ, the cold cracked fracture surface showed IG fracture followed by QC fracture, see Fig. 5a. However, when the crack initiated in the weld metal the fracture surface exhibited the IC and QC modes of fracture, Fig. 5b. However, instead of well defined smooth columnar boundary fracture surfaces, there were indications of ductile tearing (Fig. 5c) or of cleavage markings (Fig. 5d).

4. DISCUSSION

The morphology of fracture in the weld metal was different from that of the HAZ, largely because of the microstructural difference between the two regions of the weldment. The hydrogen distribution and the local concentration resulting from the welding process also influence the fracture morphology.

4.1 Susceptible Microstructure

The weld metal microstructure obtained from the cellulosic electrode in the RRC test consisted mainly of tough acicular ferrite, whereas the HAZ of the X80 steel consisted mainly of bainitic ferrite. Acicular ferrite is known to exhibit superior toughness and strength compared with bainitic ferrite. It has been well documented [2-4] that microstructures susceptible to HACC are characterised by high hardness and low toughness. Such microstructures can not plastically

accommodate stresses resulting from the weld thermal cycle and restraint. From the hardness profile, Fig. 6a, it is evident that the coarse grained HAZ and adjacent weld metal are the hardest regions of the weldment. Weld metal dilution by the base plate would be expected to raise the contents of strong carbonitride forming elements, such as Mo and Ti, in the weld bead, thereby increasing its hardenability. The progress of the crack within the weld metal towards the HAZ was in part due to the lower fracture resistance of the ferrite veins but also related to the favourable orientation of the columnar grains which was about 45° to the reaction force. The subsequent crack propagation into the HAZ is attributed to growth in a direction normal to the reaction force. Since a significant proportion of the cracking occurred through the HAZ it is inferred that the HAZ is also susceptible to cracking once the crack has been initiated in the weld metal due to hydrogen accumulation and stress concentration (in this case at the undercut).

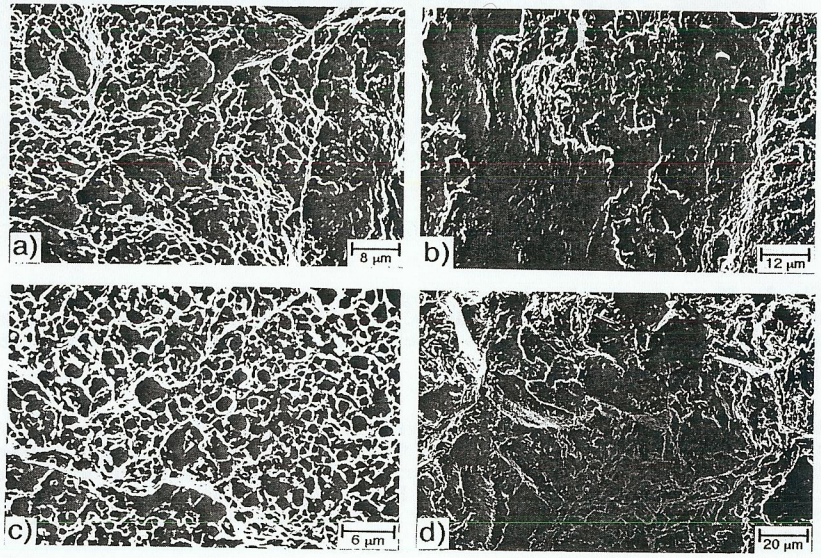

Fig. 4: Fracture morphologies of HAC cracking in high hydrogen weldments. a) fracture appearance near crack initiation site; b) fracture associated with grain boundary ferrite along columnar grains; c) fracture associated with fusion boundary; and d) fracture associated with coarse grained HAZ.

The weld metal obtained from low hydrogen electrodes in the Tekken test exhibited mainly granular bainite and some regions of acicular ferrite. The weld metal structure was harder than the HAZ, see Fig. 6b, due to the high alloy content in the E8018B2 electrode. As a result, the weld metal microstructure was more susceptible to cracking than the HAZ and cracking occurred mostly in the weld metal.

4.2 Crack Initiation and Propagation

Stress intensity and hydrogen concentration determine the morphologies of crack initiation and propagation in a weld. Based on work by Beachem [7] and Vasudevan et al [5], the schematic

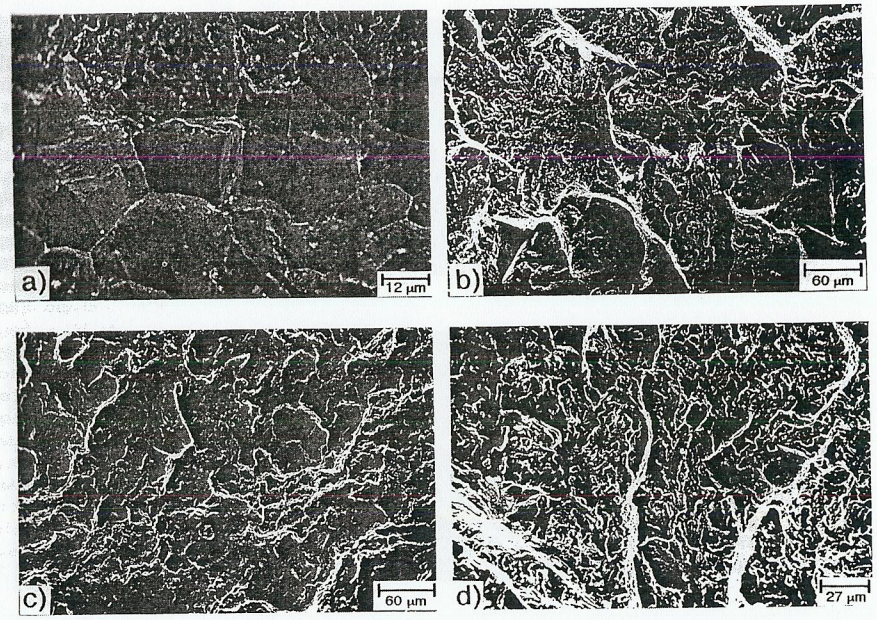

Fig. 5: Fracture morphologies of HAC cracking in low hydrogen weldments of HSLA80: a) fracture appearance near crack initiation site in HAZ; b) fracture initiation site associated with bainitic structure of weld metal; c) and d) fracture surfaces associated with columnar boundaries.

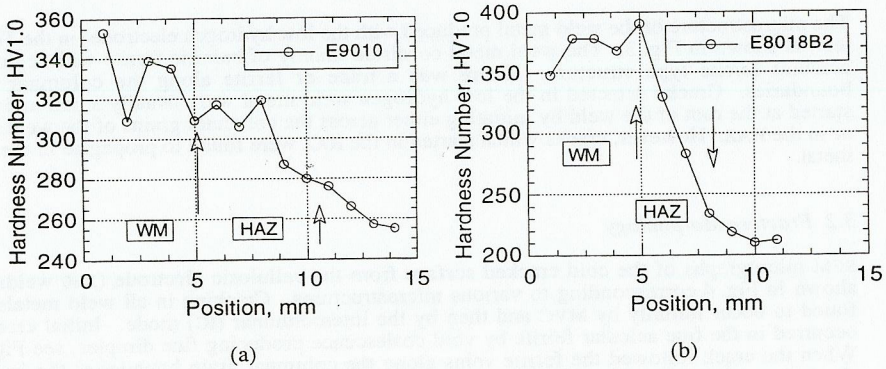

Fig. 6: Hardness profiles across welds deposited from a) the high hydrogen cellulosic E9010 electrode, b) the low hydrogen E8018B2 electrode. HAZ: heat affected zone; WM: weld metal.

diagram in Fig. 7 has been developed to explain the fracture morphology and the effect of stress intensity and crack tip hydrogen level. In the RRC test using cellulosic electrodes most cracks initiated within 5-15 minutes after welding. The hydrogen in the weld from the cellulosic electrodes can be as high as 32 ml/100 gm of weld metal. In the presence of such a high quantity of hydrogen stressed regions became highly enriched with hydrogen and as a result cracking can occur in a short period of time after the temperature of the weld drops below 200 °C.

All cracked samples exhibited ductile crack initiation from the undercuts at the weld metal surface. Under self-restraint conditions the stresses resulting from the weld thermal cycle are concentrated giving rise to a triaxial state of stress at the root of the undercuts. High stress intensity generates a large plastic zone in the hydrogen enriched acicular ferrite region ahead of the undercuts. Hydrogen in steel also lowers the yield stress [5,7] and promotes crack initiation under high stress intensity in the form of MVC. The presence of MVC at the crack initiation site of the weld metal is in agreement with other reports [5,7,8] of MVC for a relatively high hydrogen concentration in the HAZ. The relationship between stress intensity, crack tip hydrogen and cracking mode is shown schematically in Fig. 7, which is a modified form of the Beachem [7] diagram developed for hydrogen charged quenched and tempered steels and adapted by Vasudevan et al [5] for the HAZ of weldments. In the present application to the weld metal and the HAZ, complexities arise because the composition and structures are not homogeneous and the hydrogen is not uniformly distributed. In addition, the diagram is highly schematic because the time variable is not included. Despite these limitations the broad nature of the observed cracking can be rationalised by reference to the modified Beachem diagram in Fig 7 in which the boundary between IG and QC fracture is neglected. Within the hatched zone IG and/or QC can occur depending on the local restraint stress, microstructure and hydrogen content.

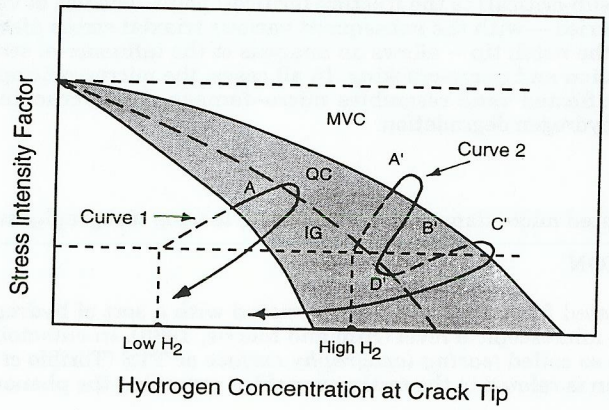

Fig. 7: Inter-relationships between stress intensity factor, and dissolved hydrogen content and cracking mode based on references 5 & 7; The lower dashed horizontal line arbitrarily represents the stress intensity at 200 °C on cooling and the two curves depict changes in stress intensity and hydrogen with cooling time below 200 °C for the low hydrogen weld metal (E8018B2) and the high hydrogen weld metal (E9010), (see text).

When the low hydrogen electrode, E8018B2, was used in the Tekken weld metal cracking test for HSLA80 steel, initiation of cracking started several hours after welding. Crack initiation

from the root notch in the Tekken test piece was in the form of IG for the HAZ and QC for the weld metal. Similar observations for low hydrogen concentrations have been reported by others [7].

In the Tekken test a sharp notch was formed at the root, where stress was concentrated as a result of welding and restraint. Hydrogen has been reported [8,9] to diffuse into regions of high triaxial stresses at which the stress intensity is very high. However, the weld metal hydrogen concentration was relatively low (8-12 ml/100 gm) and the amount of hydrogen picked up by the stressed region was not high enough to cause immediate cracking. In this case there is some incubation period [6] during which the hydrogen reaches a critical level by diffusion into triaxially stressed regions to initiate cracking by the IG or QC mode (region A of curve 1 in Fig. 7). Because low hydrogen in a susceptible microstructure can not reduce the yield strength significantly, local yielding at the root notch is energetically less favourable. Further growth of the crack in the low hydrogen weld metal was also characterised by the IC and QC modes due to the reduced amount of hydrogen ahead of the advancing crack.

In the presence of high hydrogen concentration, as in the case of cellulosic electrodes in the RRC test, the yield strength is significantly reduced and cracking initiates in the form of MVC (region A' of curve 2 in Fig 7). After travelling across the columnar grains, cracking was observed to deviate along the columnar grain boundaries (Fig. 4b) of the weld metal and the fracture was characterised by the IC mode with little sign of deformation (region B' of curve 2 in Fig. 7). As the crack grows, part of the atomic hydrogen that diffuses into the triaxially stressed region is lost as molecular hydrogen [6,11]. By the time the crack reaches an appropriately oriented columnar grain boundary, the stress intensity is reduced to a level which gives rise to a smaller plastic zone. The reduced hydrogen concentration and the smaller plastic zone resulting from the lower stress intensity at the extending crack front have been predicted to promote IG fracture with the release of built up strain energy. Although the Beachem [7] diagram indicates that QC should occur prior to IG, the weld metal structure was not homogeneous and the favourably oriented films of grain boundary ferrite have a lower fracture resistance than the acicular ferrite. As a result, IG fracture occurs in preference to QC.

Cracking at the fusion boundary in the RRC test sample occurred by MVC, nucleated by non-metallic inclusions (Fig. 4c). Hydrogen is reported to diffuse into grain boundaries and the fusion boundary at higher concentrations [9,12]. The fusion boundary was found to be a preferential site for the segregation of fine non-metallic inclusions. Inclusions are also favourable sites for hydrogen trapping [13]. On this basis the concentration of hydrogen in the fusion boundary could exceed the critical limit for extending the crack by MVC rather than QC or IG fracture. Although the stress intensity is reduced significantly by the time the crack reaches the fusion boundary, the presence of fine inclusions and the higher hydrogen concentration evidently give rise to conditions for fracture by MVC. This effect is shown schematically in Fig. 7 by the reverse loop in the hydrogen-stress trace to region C'.

Although the value of hardness is indicative of a crack prone structure, caution is needed in assessing the relative cracking susceptibilities of the weld metal and HAZ since the crack path will be strongly influenced by the state of stress in the weldment. It is evident from the Fig. 7 that for a given stress intensity the critical concentration of hydrogen for the QC and IG fracture modes is relatively low. In the high hydrogen weld, by the time the crack reaches the HAZ, the hydrogen concentration and the stress intensity have both decreased markedly. However, the hydrogen level must be high enough to extend the growing crack in the QC and IG modes (Fig. 4d and region D' of curve 2 in Fig. 7).

In summary , for the high hydrogen weld metal the cracking can be rationalised in terms of the complex path (curve 2) in Fig. 7 in which weld metal cracking starts by MVC, progresses to IG(IC) then reverts to MVC in the fusion boundary. Continuation into the HAZ is by IG and QC. The cracking path of the low hydrogen case (curve 1) in Fig. 7 does not encompass MVC but involves an IG onset for the HAZ and QC or IC for the weld metal followed by QC fracture.

5. CONCLUSIONS

The results of the microstructural and fractographic analysis of the high hydrogen weld metal from the RRC test are summarised as follows:

1. In the presence of high hydrogen content the initiation of HACC in the weld metal occurred in a short period of time and was associated with ductile fracture. High hydrogen and high stress intensity contribute to the fracture by MVC.

2. Further crack growth occurs along IC boundaries and results in loss of hydrogen. A relatively smooth fracture surface is produced with little evidence of plastic deformation. The presence of a lower hydrogen content and a smaller plastic zone resulting from a lower stress intensity appear to be associated with IC fracture.

3. Cracking along the fusion boundary was by MVC initiated by non-metallic inclusions. A high hydrogen content is likely to promote MVC type fracture.

4. Further extension of cracking through the HAZ occurred by QC and IG type fractures. The presence of a lower stress intensity and lower hydrogen content appeared to promote these types of fracture in the HAZ.

The investigation of cracking in the low hydrogen weld metal from the Tekken test samples produced the following conclusions.

1. In low hydrogen weld metal cracking occurred several hours after welding indicating that a long incubation period was required for hydrogen to reach the critical concentration for onset cracking. The crack initiation was characterised by either the IG or QC mode.

2. The path of fracture was along and across columnar grains by the IC and QC fracture modes.

ACKNOWLEDGEMENT

The authors acknowledge the research funding of the CRC for Materials Welding and Joining. The authors are also grateful to Ian Squires, Frank Barbaro and Bing Feng of FPD-BHP for providing the RRC test samples and useful information for this investigation.

REFERENCES

1. Sawhill, M. et al.: Welding Journal; 1974, **53** (12), pp 544s.
2. Boniszewski, T. and Watkinson, F.: Metals and Materials; 1973, February, pp 90 and March, pp 145.
3. Boniszewski, T. et al.: British Welding Journal; 1965, **12**(7), pp 14.
4. Boniszewski, T. and Baker, R.G.: British Welding Journal; 1965, **12**(7), pp 349.
5. Vasudevan, R. et al: Welding Journal; 1981, **60**(9), pp 155s.
6. Okuda, N. et al.: Welding Journal; 1987, **65**(5), pp 141s.
7. Beachem, C.D.: Metallurgical Transaction; 1972, **3**(2), pp 437.
8. Savage, W.F. et al.: Welding Journal; 1976, 55(11), pp 368s.
9. Alam, N. and Dunne, D.: CRC Project on Weld Metal Cracking (93-07).
10. Troiano, A.R.: Transaction of American Society of Metals; 1960, 52(1), pp 54.
11. Savage, W.F. et al.: Welding Journal; 1976, 55(12), pp 400s.
12. Yurioka, N. and Suzuki, H.: International Materials Reviews; 1990, 35(4), pp 217.